Open Archive Toulouse Archive Ouverte (OATAO)

OATAO is an open access repository that collects the work of Toulouse researchers and makes it freely available over the web where possible.

Any correspondence concerning this service should be sent to the repository administrator: staff-oatao@inp-toulouse.fr

Characterization of lead-recycling facility emissions at various workplaces: Major insights for sanitary risks assessment

G. Uzu [a,b], S. Sobanska [c], G. Sarret [d], J.J. Sauvain [e], P. Pradère [f], C. Dumat [g,h,*]

[a] *Université de Toulouse; UPS; LA (Laboratoire d'Aérologie); CNRS; 14 Av Edouard Belin; F-31400 Toulouse, France*
[b] *IRD; LMTG; F-31400 Toulouse, France*
[c] *LASIR UMR 8516, Univ Lille I, CNRS, 59655 Villeneuve d'Ascq Cedex, France*
[d] *Environmental Geochemistry Group, LGIT, UMR 5559, University J. Fourier and CNRS, BP 53, 38041 Grenoble Cedex 9, France*
[e] *IST Institute for Work and Health, 21 rue du Bugnon, 1011 Lausanne, Switzerland*
[f] *STCM, 30-32 avenue de Fondeyre, 31200 Toulouse, France*
[g] *Université de Toulouse, UPS, INP, EcoLab (Laboratoire d'écologie fonctionnelle), ENSAT, Avenue de l'Agrobiopôle, F-31326 Castanet-Tolosan, France*
[h] *CNRS, EcoLab, F-31326 Castanet-Tolosan, France*

ARTICLE INFO

ABSTRACT

Most available studies on lead smelter emissions deal with the environmental impact of outdoor particles, but only a few focus on air quality at workplaces. The objective of this study is to physically and chemically characterize the Pb-rich particles emitted at different workplaces in a lead recycling plant. A multiscale characterization was conducted from bulk analysis to the level of individual particles, to assess the particles properties in relation with Pb speciation and availability. Process PM from various origins were sampled and then compared; namely *Furnace* and *Refining PM* respectively present in the smelter and at refinery workplaces, *Emissions PM* present in channeled emissions.

These particles first differed by their morphology and size distribution, with finer particles found in emissions. Differences observed in chemical composition could be explained by the industrial processes. All PM contained the same major phases (Pb, PbS, PbO, $PbSO_4$ and $PbO \cdot PbSO_4$) but differed on the nature and amount of minor phases. Due to high content in PM, Pb concentrations in the $CaCl_2$ extractant reached relatively high values ($40\,mg\,L^{-1}$). However, the ratios (soluble/total) of $CaCl_2$ exchangeable Pb were relatively low (<0.02%) in comparison with Cd (up to 18%). These results highlight the interest to assess the soluble fractions of all metals (minor and major) and discuss both total metal concentrations and ratios for risk evaluations. In most cases metal extractability increased with decreasing size of particles, in particular, lead exchangeability was highest for channeled emissions.

Such type of study could help in the choice of targeted sanitary protection procedures and for further toxicological investigations. In the present context, particular attention is given to *Emissions* and *Furnace PM*. Moreover, exposure to other metals than Pb should be considered.

1. Introduction

In 2008, 3 840 000 tons of lead were produced worldwide [1]. Actually, lead is used for multiple applications (electronics, medicine and automobile industry); lead acid battery production constituting nowadays its main world use (75%). In Europe, 4800 tons of lead were released in 2007 in the atmosphere [2]: lead is mainly emitted by industrial activities including smelters for lead production and recycling [3].

Due to economical and environmental considerations, the majority of lead acid batteries are recycled. At workplaces of lead-recycling facilities, particles (PM) enriched mainly with lead (and generally few minor metals) are emitted. These PM of various sizes including PM_{10}, $PM_{2.5}$, PM_1 and $PM_{0.1}$ (aerodynamic diameter of particle matter respectively below 10, 2.5, 1 and 0.1 μm) are a source of lead exposure for workers via inhalation and ingestion and thus, considered as health hazards [4]. Moreover, diffuse particles can impact surrounding soils and vegetation [5]. Sanitary protections have been settled in these facilities to limit workers exposure, particularly concerning fine particles inhalation. Since 2007, in Europe, the REACH legislation imposes to realize "exposure

scenarios" in order to recommend adapted working conditions. Moreover, lead was classified as an element of very high concern (SVHC) in European policies.

According to European PM present regulation, monitoring of industrial emissions is limited to the measurement of total lead amounts in total suspended particles (TSP), including PM_{10} and $PM_{2.5}$ [6]. However, these measurements are insufficient because they do not provide information on the bioavailability, bioaccessibility and potential toxicity of particles [7]. According to Ruby et al. [8], potential effects on health mainly depend on size distribution and Pb chemical speciation which govern its availability in biological fluids and soils. Ruby et al. [9] showed that gastric bioaccessibility of lead strongly increased for particles under diameter of 2.4 μm. The lead speciation may evolve after emission due to physico-chemical reactions occurring in the atmosphere, leading to secondary phases with different toxicities and reactivities compared to the original particles. In this context, the determination of metal speciation and process emissions characterization, both after collection and after ageing, are necessary to better assess sanitary risks.

In a previous study, we have characterized $PM_{10-2.5}$ and $PM_{2.5-1}$ fractions of channelled emissions (materials representative of outdoor emissions) from a secondary smelter recycling lead batteries [10]. We have also studied the transfer of lead in plants grown on a soil spiked with the PM [10], and the foliar transfer of lead in plants grown in the courtyard of the smelter [11]. This facility also emits indoor fugitive diffuse emissions, which are not channelled. At workplaces, people are exposed to these particles, which remain to be characterized [12]. Most available studies on lead-containing PM dealt with the environmental impact of outdoor particles [13]. Few of them were focused on PM collected at various workplaces [14,15] although indoor PM have been found to induce biological effects on workers [12].

The objective of this study was to characterize physically and chemically the Pb-rich process particles from different origins in a recycling plant, with a special focus on lead speciation, exchangeability and toxic potential. These data were combined, so as to evaluate the variability of particle properties among working units in the plant and to propose a classification in terms of risk for human health. Since PM from process emissions by lead smelters generally display a large heterogeneity in size, chemical composition and speciation [16], a multi-scale characterization from bulk analysis to the level of individual particle was needed. The particle size distribution, the amount of inhalable particles (<10 μm) and total elemental content after acid digestion were determined. According to Ettler et al. [17], leaching tests help to evaluate possible environmental effects related to the release of contaminants from smelter emissions, fly ash, or air-pollution-control residues. By analogy to phytoavailability tests used for lead present in soils impacted by atmospheric fallouts [18], an estimation of their exchangeability performed as a first step towards an evaluation of their toxic potential [19]. The exchangeable fraction was estimated by the simple and currently used 0.01 M $CaCl_2$ in vitro test [20]. Among the various available procedures, only $CaCl_2$ extraction is a correct indicator of phytoavailability, simultaneously for Pb, Cd, Zn and Cu [21]. Several physical techniques providing the description of lead speciation in the particles were then combined. Environmental scanning electron microscopy (ESEM) provided insights on the morphology of individual particles, which can influence their transfer towards biosphere. The identification of crystallized compounds with an abundance superior to 5% in weight was obtained by X-ray diffraction (XRD). Average Pb speciation was obtained by Pb L_{III}-edge extended X-ray absorption fine structure (EXAFS) spectroscopy. Finally, Raman microspectrometry (RMS) was used to determine lead speciation within individual particles with a lateral micrometer resolution. These data were

then discussed in light of the estimated bioavailability of bulk particles.

2. Experimental

2.1. Particle sampling and size separation

A secondary lead smelter, which currently recycles batteries, was chosen as representative of the smelter metal industry. The context and plant process had been previously described [10]. After 3 months of deposit, total suspended particles (PM_{tot}) were collected in two working units, as described by Uzu et al. [10] by surface wiping. The working units included (i) the smelter where lead pastes from broken batteries are processed in rotary furnaces at 1200 °C, particles noted *Furnace PM* and (ii) the refinery where lead is purified or enriched from other trace metals, particles noted *Refining PM*. PM_{tot} measured in the ambient air of the two working units was within a range of 100–700 μg m^{-3} and 70–200 μg m^{-3}, respectively. Yearly mean lead concentration measured in emitted PM_{10} (collected by Partisol 2025) sampled at a distance of 100 m from the factory is within 0.4–0.6 μg m^{-3}. In addition, to perform a global study of risks assessment due to PM exposure, PM from channeled emissions were also sampled (particles noted *Emission PM*). These Emission PM are implied both in potential indoor and outdoor impacts. According to Sobanska et al. [16], filters do not modify lead speciation contained in the dust, but retain preferentially the larger dust particles (>10 μm). Therefore, in order to collect sufficient amounts of particles, *Emission PM* were sampled before the electrofilters used in the facility.

As particles from process are highly heterogeneous in size, they were size-segregated through resuspension in Teflon bag [22] and collected by impaction using a PM_{10} Dekati inertial impactor. This cascade impactor consists in two successive stages with aerodynamic cut-off diameters of 10 and 2.5 μm when operated at 10 L min^{-1} airflow, allowing the collection of two particle size fractions, i.e., 10–2.5 μm for the coarse fraction ($PM_{10-2.5}$) and 2.5–1 μm for the fine fraction ($PM_{2.5-1}$). Size-segregated process particles were then transferred to sealed opaque containers and stored in a cool (4 °C) dark place with Merck desiccant until analyses.

2.2. Characterization of particles

Most of chemical and physical characterizations were immediately done after PM collection. Particles after 1-year storage in plastic bags in the dark at 4 °C with a desiccant were re-analyzed by XRD to assess a potential ageing processes and finally by EXAFS spectroscopy (due to beam time schedule).

2.2.1. Size distribution of particles
Size distribution of particles (bulk samples, size < 300 μm, noted PM_{tot}) was determined by laser granulometric analyses using a Malvern Mastersizer S, allowing for particle size measurements in the range of 0.05–900 μm. 50 mg of dust samples were dispersed in alcohol to avoid potential hydrophobic agglomeration, then sonicated during 10 min [30]. The accuracy of the measurement was checked with SiO_2 nanoparticles.

2.2.2. Total elemental contents
Total elemental contents of PM_{tot}, $PM_{10-2.5}$ and $PM_{2.5-1}$ were measured using ICP-MS (7500 ce, Agilent Technologies Santa Clara, CA, USA) after heated digestion with standard acid (HNO_3, HCl and HF, Suprapur, Merk) in a PTFE vessel and filtration (Millex syringe 0.22 μm). Indium/rhenium was added as an internal standard. Detection limits were below 10 ng L^{-1} and analytical errors less than 5%. Carbon, sulfur and oxygen were determined with an

elemental analyser with coulometric–catharometric and infrared cells detection (Vario Micro).

2.2.3. Major lead crystallized compounds

Major lead crystallized compounds were identified by X-ray diffraction on PM samples immediately after collection. In addition, a new XRD analysis was performed upon *Emissions PM$_{tot}$* and *Furnace PM$_{tot}$* after 1-year storage to check for potential ageing effects. XRD patterns were recorded with an INEL diffractometer equipped with a curved detector CPS 120 and Co (Kα) radiation allowing a 120°/2θ detection. Diffractograms were acquired using a rotating sample holder to avoid orientation effects. Crystallized compounds were identified by comparison with the referenced XRD patterns from the Joint Committee on Powder Diffraction Standards (JCPDS) database.

2.2.4. Major lead chemical forms

Major lead chemical forms in *Emission PM* were determined by Pb L$_{III}$-edge EXAFS spectroscopy. Spectra were recorded at the French synchrotron facility SOLEIL (St Aubin, France) on the SAMBA beamline equipped with a Si(1 1 1) double crystal monochromator. The spectra for PM samples and for Pb reference compounds were recorded in transmission mode at room temperature after dilution in boron nitride. After normalization, PM spectrum was fitted by linear combinations using a library of standard spectra recorded at room temperature during the experiment, including metallic Pb, PbS, PbSO$_4$, PbO·PbSO$_4$, α- and β-PbO, PbCO$_3$ and Pb$_3$(OH)$_2$(CO$_3$)$_2$, or provided by Manceau et al. [23] and Morin et al. [24], and Pb sorbed ferrihydrite (Pb-FeOOH) at various Pb loadings provided by Scheinost et al. [25]. The fit quality was evaluated based on normalized sum squares (*NSS*) residual parameter ($NSS = \sum[k^2\chi_{exp} - k^2\chi_{fit}]^2 / \sum[k^2\chi_{exp}]^2 \times 100$).

2.2.5. Morphology of individual particles

Morphology of individual particles was observed 6 months after sampling from secondary electron images recorded by an Environmental Scanning Electron Microscope (ESEM; Quanta 200 FEI instrument). ESEM was equipped with an Energy Dispersive X-ray (EDX) spectrometer (Quantax EDX detector Rontec). ESEM-EDX was operated at 10–25 kV in a low vacuum mode. Particles were deposited on carbon substrates and analyzed without further preparation.

2.2.6. Molecular identification of species

Molecular identification of species within individual particles was performed 6 months after sampling by Raman microspectrometry (RMS) using a LabRAM confocal spectrometer (Jobin Yvon, Horiba Gr, France). Raman backscattering was excited at 632.8 nm by an internal, air-cooled, linearly polarized helium–neon laser. The laser beam was focused on particle surfaces through an optical objective (Olympus objective, 100×, 0.9 NA), given a lateral resolution (*XY*) of about 1 μm^2. The power delivered to the surface of particle was less than 8 mW. A liquid nitrogen-cooled CCD (Jobin Yvon, 2048 × 512 pixels) was used for the detection of backscattered light. Glass plates with the impacted particles (PM$_{10-2.5}$ and PM$_{2.5-1}$ samples) were directly mounted on the microscope stage without any further preparation. Data acquisition consisted in recording many spectra in a point-by-point scanning mode with 1 μm as a minimum step, one accumulation and 30 s spectrum acquisition time. To assess representative molecular composition issued from particles analysis, we recorded large areas of every samples (60 μm × 30 μm) in an automated mode. So, for each area, a total of 1800 spectra were acquired and simultaneously treated using Multivariate Curve Resolution (MCR) to extract the main spectrum from the whole data set. Further details about data

Table 1
Size distribution (volumetric percentage) of PM emitted by the Pb recycling process.

	Refining PM	Furnace PM (vol.%)	Emissions PM
<1 μm	2.4	7.4	**21.0**
1–2.5 μm	2.1	6.3	**19.9**
2.5–10 μm	**16.7**	**14.0**	<u>50.0</u>
10–30 μm	<u>56.4</u>	<u>38.4</u>	8.2
30–100 μm	**22.4**	**30.2**	0.9
>100 μm	<LD	3.7	<LD

The main size fraction is underlined and secondary is in bold characters. <LD: lower than detection threshold (LD = 0.01 vol.%). Results are averaged upon five replicates and standard deviations do not exceed 0.2%.

treatment can be found elsewhere [26]. Identification of molecular species was obtained by comparison (Raman band positions and relative intensities) between extracted Raman spectra and reference spectra referenced in the Spectral Library Search ID 301 software.

2.3. Estimation of metal exchangeable fractions and health risk assessment

Exchangeable fractions of metals in process particles were estimated by CaCl$_2$ chemical exchange. Following the procedure described by Houba et al. [19], freshly collected particles were mixed with 0.01 M CaCl$_2$ solution in 1:10 (g:mL) ratio. Extraction was carried out on 1 g of various PM samples (PM$_{tot}$, PM$_{10-2.5}$ and PM$_{2.5-1}$) in triplicates. Two hours extractions were performed at 20 °C in 50 mL polypropylene centrifugation tubes placed on a shaker table (Heidolph promax 1020) at 50 oscillations/min during. The filtered supernatant (0.22 μm) was acidified at 2% with bidistilled HNO$_3$ (15 N, suprapur 99.9%) and stored at 4 °C, before analysis by ICP-OES (Thermo IRIS INTREPID II XDL, Waltham, MA, USA). Detection limits were below 100 μg L^{-1} in ICP-OES analysis and analytical errors less than 5%.

In order to evaluate potential hazard of aerosols generated during a typical working shift (8 h) at the two different processes (*Furnace* and *Refining*), the total deposited dose in the lungs were calculated for the different metals and metalloids. In addition, their distribution between the tracheo-bronchial (thoracic) and alveolar part of this organ were assessed. Calculation were based on typical PM$_{tot}$ concentrations of 350 μg m^{-3} and 150 μg m^{-3} respectively measured at *Furnace* and *Refining*, with their corresponding size distributions given in Table 1. The inhalable convention [27] was used to determine the amount of particles entering the lungs; the tracheo-bronchial fraction being obtained after subtracting the alveolar fraction from the total inhalable fraction. We hypothesised that workers inhale 9.6 m^3 air during a shift in case of moderate activity [28] without any personal respiratory protection; also that metallic compositions of the PM$_1$ and PM$_{2.5-1}$ were the same. Finally, the CaCl$_2$ extraction test was considered as representative of the metal load (free ions and complexes) to which organs or cells are exposed (bioaccessible fraction). The deposited amount in the tracheo-bronchial and alveolar region has been estimated for each particle size using the Multiple-Path Particle Dosimetry model (MPPD vers 2.0 [29]). Thus, we estimated an average deposition of 7.6% in the tracheo-bronchial compartment against 12.3% in the alveolar one.

3. Results

3.1. Size distributions

Table 1 displays the observed size for the different bulk process PM samples collected at the three places, i.e., furnace, refining and emissions. Granulometry distribution is expressed as volumet-

Table 2
Elemental total mass contents (mass of element/total mass expressed in %) of PM emitted by the Pb recycling process.

	Al	As	Cd	Cu	Fe	Na	Ni	Pb	Sb	Zn	S	Cl	C	O
Refining														
PM_{tot}	0.07	0.3	0.2	0.6	1.3	2.2	0.5	41	1.9	0.2	2.9	n.d.	2.2	20.5
$PM_{10-2.5}$	0.08	0.6	0.2	0.7	1.4	5.9	0.3	32	2.3	0.4	7.2	0.35	4.1	19.2
$PM_{2.5-1}$	0.09	0.5	0.2	0.7	1.4	8.9	0.2	32.3	2.1	0.4	7.4	n.d.	4.3	20
Furnace														
PM_{tot}	0.1	0.06	0.2	0.2	5.7	6.8	0.08	25.7	0.55	0.2	2.8	n.d.	4.6	20.1
$PM_{10-2.5}$	0.07	0.08	0.4	0.2	4.5	10.3	0.05	45.2	0.6	0.3	7.6	0.54	6.5	21
$PM_{2.5-1}$	0.05	0.08	0.7	0.1	2.1	8.3	0.02	38	0.49	0.4	8.2	n.d.	5.1	20.1
Emissions														
PM_{tot}	0.02	0.09	2.7	0.09	1.2	5	0.02	33.4	0.18	0.7	3.3	n.d.	1	15
$PM_{10-2.5}$	0.005	0.08	2.3	0.06	0.4	4	0.009	26.7	0.14	0.5	7.4	1.93	1.2	15.1
$PM_{2.5-1}$	0.001	0.09	2.5	0.05	0.1	3.2	0.004	27.3	0.13	0.5	7.8	n.d.	1.2	14.9

n.d. stands for not determined. Results are averaged upon three replicates, standard deviations not exceeding 0.1%.

Table 3
Minerals identified by powder XRD.

Samples	Minerals
Refining	
PM_{tot}	Pb^0, PbS, $PbO \cdot PbSO_4$, $Pb(ClO_4)_2$, $Pb_2As_2O_7$, $CdSO_4$, CdS, Na_2SO_4
PM_{10}	Pb^0, PbS, $PbO \cdot PbSO_4$, $Pb(ClO_4)_2$, $Pb_2As_2O_7$, $CdSO_4$, CdS, Na_2SO_4, ZnO
$PM_{2.5}$	Pb^0, PbS, $PbO \cdot PbSO_4$, $Pb(ClO_4)_2$, $Pb_2As_2O_7$, $CdSO_4$, CdS, Na_2SO_4, ZnO
Furnace	
PM_{tot}	Pb^0, PbS, $PbO \cdot PbSO_4$, $Pb(ClO_4)_2$, $Pb_2As_2O_7$, $CdSO_4$, CdS, Na_2SO_4
PM_{10}	Pb^0, PbS, $PbO \cdot PbSO_4$, $Pb(ClO_4)_2$, $Pb_2As_2O_7$, $CdSO_4$, CdS, Na_2SO_4, ZnO, $ZnSO_4$
$PM_{2.5}$	Pb^0, PbS, $PbO \cdot PbSO_4$, $Pb(ClO_4)_2$, $Pb_2As_2O_7$, $CdSO_4$, CdS, Na_2SO_4, $2PbO \cdot PbSO_4$
Emissions	
PM_{tot}	Pb^0, PbS, $PbO \cdot PbSO_4$, $Pb(ClO_4)_2$, $CdSO_4$, $Cd(ClO_4)_2$, Na_2SO_4
PM_{10}	Pb^0, PbS, $PbO \cdot PbSO_4$, $Pb(ClO_4)_2$, $CdSO_4$, $Cd(ClO_4)_2$, Na_2SO_4
$PM_{2.5}$	Pb^0, PbS, $PbO \cdot PbSO_4$, $Pb(ClO_4)_2$, $CdSO_4$, $Cd(ClO_4)_2$, Na_2SO_4, FeS_2

ric percentage (for equivalent spheres) of PM samples. All particle samples show a wide size distribution ranging from 0.05 μm to 100 μm. Results let appear large differences between workplaces and channeled emissions: the two workplaces present a majority of coarse particles (between 10 and 100 μm), whereas *Emissions PM* display a majority (90%) of <10 μm particles.

3.2. Total elemental contents

Elemental composition of particles from the three sources as function of particle sizes is shown in Table 2. All results (expressed in wt%) are averaged over the three replicates for each sample (i.e., PM_{tot} $PM_{10-2.5}$ and $PM_{2.5-1}$). Lead is the major element in all PM,

Table 4
Determination of main species observed by Raman microspectrometry.

	Phases identified
Refining	
PM_{tot}	**$4PbO \cdot PbSO_4$**, **$PbSO_4$**, **α-PbO**, **Na_2SO_4**, $PbCO_3$, $Pb_3(CO_3)_2(OH)_2$, $(Fe,x)_3O_4$
PM_{10}	**$4PbO \cdot PbSO_4$**, **$PbSO_4$**, **α-PbO**, **Na_2SO_4**, $PbCO_3$, $Pb_3(CO_3)_2(OH)_2$, $(Fe,x)_3O_4$
$PM_{2.5}$	**$PbO \cdot PbSO_4$**, **$PbSO_4$**, $PbCO_3$, **α-PbO**, **Na_2SO_4**, α-Fe_2O_3
Furnace	
PM_{tot}	**$PbO \cdot PbSO_4$**, **$PbSO_4$**, **α-PbO**, **Na_2SO_4**, $PbCO_3$
PM_{10}	**$PbO \cdot PbSO_4$**, **$PbSO_4$**, **α-PbO**, **Na_2SO_4**, $PbCO_3$, β-PbO, $ZnSO_4$, α-Fe_2O_3
$PM_{2.5}$	**$PbO \cdot PbSO_4$**, **$PbSO_4$**, **α-PbO**, **Na_2SO_4**, $PbCO_3$, α-Fe_2O_3, $(Fe,Zn)_3O_4$, Fe_3O_4
Emissions	
PM_{tot}	**$PbO \cdot PbSO_4$**, **α-PbO**, β-PbO, **Na_2SO_4**, $(Fe,Zn)_3O_4$
PM_{10}	**$PbO \cdot PbSO_4$**, **α-PbO**, **$PbSO_4$**, $PbCO_3$, **Na_2SO_4**, $ZnSO_4$, $CaSO_4$
$PM_{2.5}$	**$xPbO \cdot PbSO_4$** $x = (1,2,3)$, **α-PbO**, **$PbSO_4$**, **Na_2SO_4**, $ZnSO_4$

Major compounds in bold characters.

accounting for 25–41% wt in PM_{tot} samples. Other metals and metalloids such as As, Cd, Cu, Fe, Ni, Sb and Zn were also detected in all PM_{tot} samples. In addition, Na, Cl, S and C were systematically observed in samples, up to 10 wt%. In order to evaluate possible segregation of metals as a function of particle size, an enrichment factor (EF) was calculated following the equation: $EF_i = (C_i)_{PM_x} / (C_i)_{PM_{tot}}$, where EF_i is the enrichment factor for element i; $(C_i)_{PM_x}$ is the concentration of element i measured in fraction PM_x (with $x = 10$ or 2.5 μm) and $(C_i)_{PM_{tot}}$ is the concentration of element i in the fraction PM_{tot} (Table 3). Thus, $EF_i > 1$ indicates an enrichment. When compared to PM_{tot}, a slight metal enrichment in coarse and fine fractions of *Furnace and Refining PM* was observed. *Furnace* $PM_{10-2.5}$ and $PM_{2.5-1}$ samples were enriched in Cd, Na, Pb, Zn and S, while enrichment in Na, As and Zn was observed in $PM_{10-2.5}$ and $PM_{2.5-1}$ at *Refining* site. No metal enrichment was observed in channeled emissions.
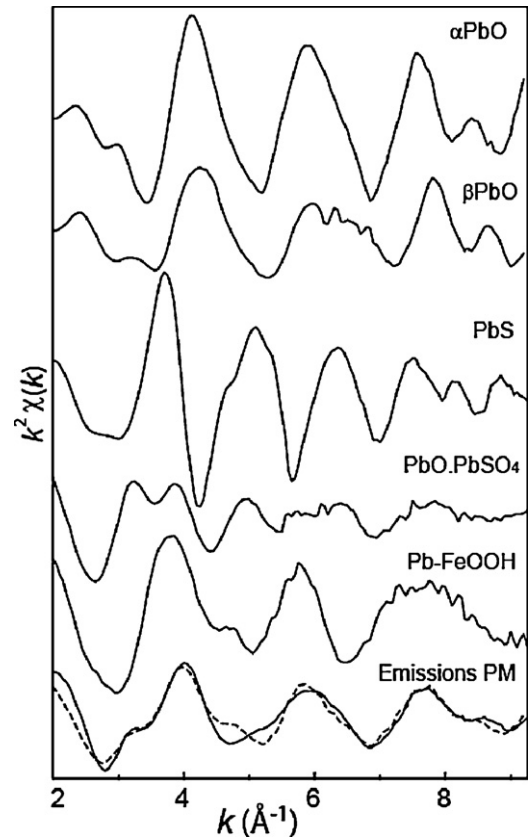
Fig. 1. Pb L_{III}-edge EXAFS spectra for aged *Emissions PM* and reference compounds. Dashed line: linear combination fit.
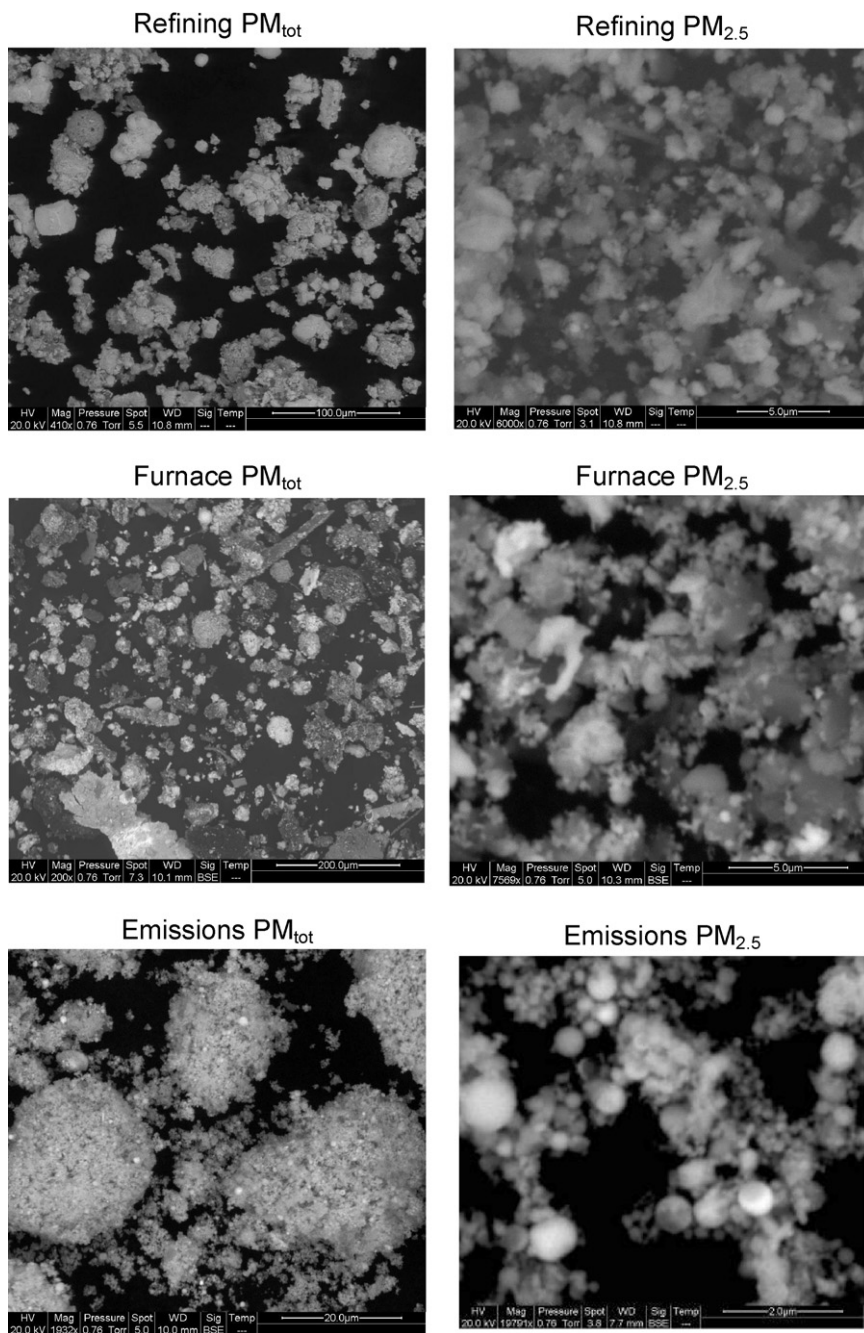
Refining PM_tot   Refining PM_2.5

Furnace PM_tot   Furnace PM_2.5

Emissions PM_tot   Emissions PM_2.5

Fig. 2. SEM observations on PM from different origins.

3.3. Global speciation results

XRD patterns for PM_{tot}, $PM_{10-2.5}$ and $PM_{2.5-1}$ from the various sources contain numerous peaks corresponding to several crystallized species. Table 4 presents the major phases identified.

Regardless of their origin, freshly deposited particles are mainly composed of metallic sulfates, sulfides, oxides, oxisulfates and perchlorates. In addition, sodium sulfate ($NaSO_4$) is clearly identified in all samples. Major lead species include elemental Pb, PbS, $PbSO_4$, and oxysulfates $PbO·PbSO_4$ (lanarkite) and $2PbO·PbSO_4$. These species were previously observed in *Emissions PM* [10,11]. These present results show no significant difference in Pb species between channelled emissions and the two workplaces.

XRD analysis of 1-year old PM indicated that *Emissions PM_tot* and *Furnace PM_tot* did not contain Pb^0 anymore, and major Pb species included $PbO·PbSO_4$ and PbO. Fig. 1 displays Pb L_{III}-edge EXAFS spectra for reference compounds and for aged *Emission PM*. The best fit was obtained with 36% $PbO·PbSO_4$ + 28% Pb-FeOOH + 21% αPbO + 13% βPbO (NSS = 0.13). Other fits of equivalent quality were obtained with slightly different distributions (NSS = 0.14–0.16). Overall, the distribution of Pb species in *Emissions PM* could be described as 30–40% $PbO·PbSO_4$, 20–30% αPbO, 20–30% Pb-FeOOH, 0–10% βPbO and 0–10% PbS.

3.4. Individual particle analysis

ESEM observations revealed morphological differences between the different collected samples (Fig. 2). For PM_{tot} samples, *Emissions PM* exhibit large aggregates (diameter 20 μm) composed of micrometer- and nanometer-sized balls, whereas *Furnace* and

Table 5
Calculated metal enrichment factors (EF) in $PM_{10-2.5}$ and $PM_{2.5-1}$ compared to PM_{tot}.

	Al	As	Cd	Cu	Fe	Na	Ni	Pb	Sb	Zn	S	Cl	C	O
Refining														
EF $PM_{10-2.5}/PM_{tot}$	1.1	2.0	1.0	1.2	1.1	2.7	0.6	0.8	1.2	2.0	2.5	n.d.	1.9	0.9
EF $PM_{2.5-1}/PM_{tot}$	1.3	1.7	1.0	1.2	1.1	4.0	0.4	0.8	1.1	2.0	2.6	n.d.	2.0	1.0
Furnace														
EF $PM_{10-2.5}/PM_{tot}$	0.7	1.3	2.0	1.0	0.8	1.5	0.6	1.8	1.1	1.5	2.7	n.d.	1.4	1.0
EF $PM_{2.5-1}/PM_{tot}$	0.5	1.3	3.5	0.5	0.4	1.2	0.3	1.5	0.9	2.0	2.9	n.d.	1.1	1.0
Emissions														
EF $PM_{10-2.5}/PM_{tot}$	0.3	0.9	0.9	0.7	0.3	0.8	0.5	0.8	0.8	0.7	2.2	n.d.	1.2	1.0
EF $PM_{2.5-1}/PM_{tot}$	0.1	1.0	0.9	0.6	0.1	0.6	0.2	0.8	0.7	0.7	2.4	n.d.	1.2	1.0

Refining PM contain larger sizes individual particles (diameter ranging between 10 and 200 μm) and various shapes, i.e., cubes and needles (more interpretation on morphology can be found elsewhere [10]). Raman microspectrometry enabled identification of minerals at the scale of individual particles (Table 5). Scanning of a large area of sample (300 μm²) by automated analysis allowed the detection of both minor and major components in a large number of particles. Each analyzed zone (about 1 μm²) generally contained a mixture of several minerals. As previously observed in *Emissions PM* [10,11], for all samples, xPbO·PbSO₄ (with x = 1, 2 or 3), PbSO₄, α-PbO and Na₂SO₄ were the most frequently observed phases. In PM_{tot} samples, a large number of particles were made of aggregates, composed of PbSO₄ mixed with Na₂SO₄. As samples were analyzed by RMS 6 months after collection, changes in speciation may have occurred. Indeed, minor components of lead (such as PbCO₃) were observed with this technique.

3.5. Exchangeability of metals in particles and evaluation of the dose deposited in the lungs

Results of CaCl₂ extractions carried out for 10 metals and metalloids are displayed in Fig. 3. Regardless of the PM origin, the percentages of exchangeable lead were relatively low: highest extractions were observed for *Emissions PM* (0.015%), while *Furnace* and *Refining PM* were <0.01%. Still, lead concentrations in the extractant were relatively high (up to 40 mg L⁻¹ for *Emissions PM*). Several significant features were observed: (i) lead and cadmium exchangeability was higher for *Emission PM* than for *Furnace* and *Refining* workplaces; (ii) except for As and Sb, metal exchangeability generally increased when size decreased; (iii) As and Cu were under 0.001% in *Emissions*; (iv) whatever the source of particles, the less exchangeable metal was Fe (<0.001%) followed by Pb (<0.015%). In *Emissions PM* samples, regardless of the size, the most exchangeable metal was Cd (up to 18% in $PM_{2.5-1}$), followed by Ni and Zn.

Deposited doses of the different elements in the two different lung compartments (tracheo-bronchial and alveolar) at *Furnace* and *Refining* workplaces are shown in Fig. 4. These deposited doses correspond to about 18% of the total inhaled mass. As expected, lead is the dominant deposited element at both workplaces. Distribution of metallic elements in the different lung compartments is different between *Furnace* and *Refining* places. On average, at *Furnace*, about 2/3 of inhaled elements are found in the alveolar region against 1/3 in the tracheo-bronchial space, whereas for *Refining*, this ratio is about 1/2. From Fig. 4, it is also clear that lung burden with minor elements is not the same at these two workplaces. For example, workers inhale larger amounts of Cd and Fe at *Furnace* when compared to *Refining*. When looking at the exchangeable fractions of deposited doses, considered as representative of bioaccessible amounts, it is interesting to observe that the metal of most concern is no longer Pb, but Cd at the *Furnace* and Cu at *Refining* workplaces.

4. Discussion

4.1. Total content of metallic elements, distribution in size fractions and morphology of process particles

Size distributions strongly differed between workplaces and channeled emissions. 90% of *Emissions PM* had a diameter below 10 μm. The main part of *Emissions PM* is thus likely emitted in the environment according to Sobanska et al. [16]. Inhalable fraction (<10 μm) represents 21%, 28% and 90% in *Refining PM*, *Furnace PM*, and *Emissions PM* samples, respectively. The proportion of PM₂.₅, which represent an additional hazard for deep lung penetration [30,31], increases from 2% at *Refining PM* to 6% in *Furnace PM* and 14% at *Emissions PM*. Since workers are protected from dust with FFP3 (Norm EN149) masks blocking 98% of particles larger than 0.6 μm in diameters, their final exposure is sharply decreased. However, this protection is still not total, since fine emitted particles represent a potential risk for unprotected humans and the environment in the surroundings, as well.

Some general trends were observed in terms of total elemental contents: (i) all PM_{tot} samples contain extremely high Pb levels (from 25 to 41 wt%); (ii) secondary metals and metalloids (As, Cd, Cu, Fe, Ni, Sb and Zn) were detected; (iii) in addition, up to 10 wt% Na, S, Cl and C were observed in the samples. However, each particle type displays a specific elemental signature. *Furnace PM* samples are characterized by their high contents in C (4.6 wt%), Fe (5.7 wt%) and Na (6.8 wt%). Carbon and iron are found in a higher proportion because they are added in this unit to improve the reducing step and as a desulfurising agent respectively. Sodium carbonate (Na₂CO₃) is added in the furnace in order to decrease the melting point of the slag. *Refining PM* contains the highest amounts of As (0.3 wt%), Cu (0.6 wt%), Ni (0.5 wt%), Pb (41 wt%) and Sb (1.9 wt%). This was expected since in the refining unit, Pb is mixed with other metals to produce alloys. Cd and Cl are more concentrated in *Emission PM* (2.7 and 2 wt%, respectively). Presence of Cd is attributable to the unwanted occasional presence of Cd–Ni batteries and the enrichment of *Emissions PM* with this element could be due to its volatility (boiling point Cd: 765 °C). Chloride can originate from PVC separators decomposition and batteries box.

No metal enrichment was observed in channeled emissions which is consistent with the fact that 90% of the particles have diameters below 10 μm (so PM_{tot} concentrations are close to those of PM₁₀₋₂.₅/₂.₅₋₁). However, certainly due to chemical heterogeneity of samples, the calculated EF factors show slight variations (0.1–4) (Table 3). During the process of lead isolation (in *Furnace*) and refining, several mechanisms are involved such as melting, volatilization, formation of solid solutions, co-precipitations, etc. [3]. They can induce changes in particulate elemental contents with no simple relationship with particle size or sources. Moreover, about transfers or toxicity towards the biosphere, competition or/and synergetic effects could be promoted due to the numerous metals present in particles [32]. As a consequence, these data on
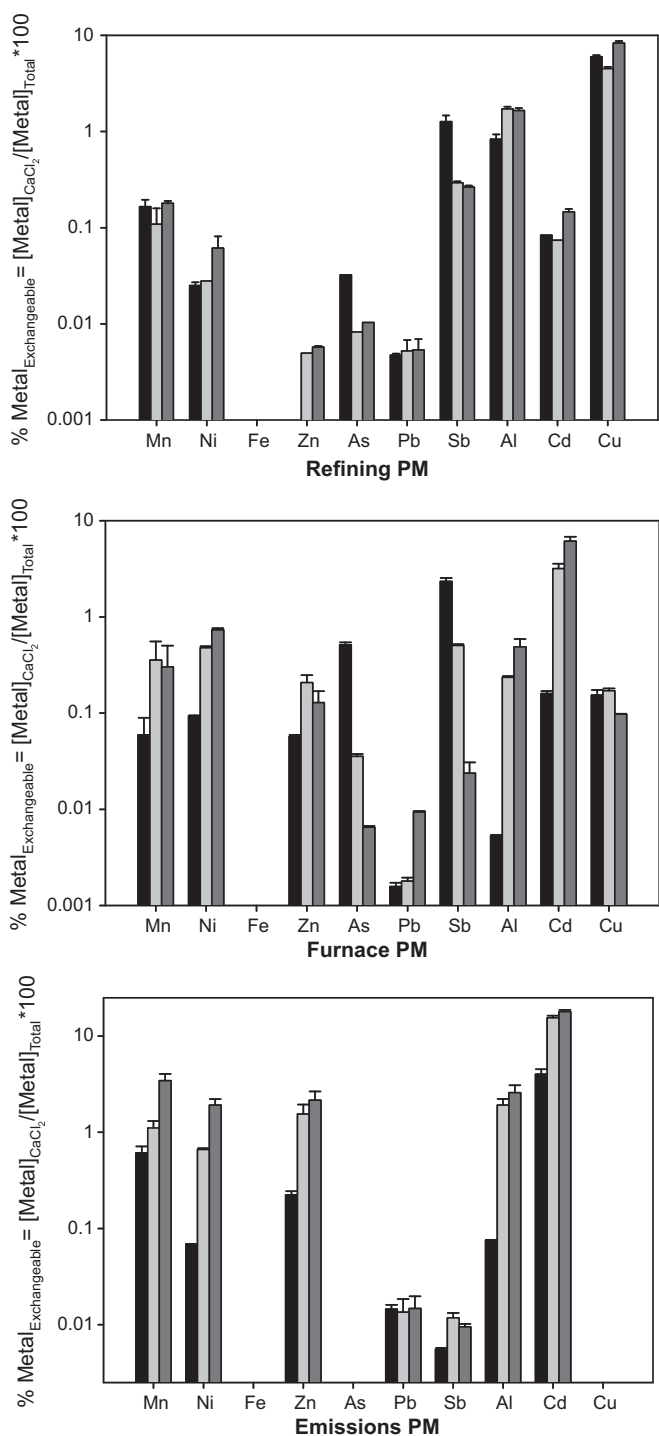
Fig. 3. Results of CaCl$_2$ (0.01 M) extractions for refining, furnace and *Emissions PM*, expressed as the percentages of total metal content: (■) PM$_{tot}$, (▨) PM$_{10}$ and (▧) PM$_{2.5}$.

total elemental concentrations are a starting point in the study of particles, which need to be supplemented by data on structure, mineralogy and metals (bio)avaibility.

SEM observations of PM samples revealed differences related to particle sizes and workplaces. As shown in Fig. 2, numerous spherical nanoparticles were observed only in *Emissions PM$_{2.5}$*. Such micrometer-sized Pb-containing balls are likely due to fusion process. In addition to size, it is well known that particle shape can influence their biological effects (due to steric, solubility or diffusion differences) [10].

Finally, low sums were observed for elemental total mass contents (mass%) of PM emitted by the Pb recycling process (Table 2). Several hypotheses could explain these observations: (i) an incomplete digestion could explain this fact, we may have under-estimate Ca, Si or Al, refractory elements which are not likely soluble in HNO$_3$; however, we used HF, the strongest acid to achieve the digestion; (ii) the dosage of oxygen could lack of precision and inorganic carbon may have been under-estimated; and (iii) some elements such as N and P were not measured although they likely contribute to the sum.

4.2. Global and individual particle metal speciation in relation with process steps and ageing

Global speciation results (XRD and EXAFS) were in agreement with elemental bulk analysis. Major lead species include elemental Pb, PbS, PbSO$_4$, and the oxysulfates PbO·PbSO$_4$ (lanarkite) and 2PbO·PbSO$_4$. These compounds are consistent with the composition of lead acid batteries since Pb$^{(0)}$ and PbO$_2$ compose the electrodes and H$_2$SO$_4$ corresponds to the electrolyte. Lead sulfates are accumulated on the electrode surfaces during the reduction–oxidation cycles of working batteries. In addition, lanarkite is also a product of atmospheric oxidation of PbS and PbSO$_4$ [22]. Fe contents are low compared to Pb ones (Table 2). Therefore, presumed presence of 28% of Pb-FeOOH from EXAFS analysis is unlikely. This may indicate the presence of other Pb sorbed species for which we do not have the corresponding reference spectra. Despite such uncertainty, it is clear from XRD and EXAFS results that Pb speciation was modified after 1 year, despite the relatively protective storage conditions. This ageing effect, leading to the formation of oxides, oxysulfates and sorbed lead species, suggests an increase in (bio)accessibility of particle metals. This is in agreement with fast PM weathering observed after emission in the atmosphere [33] and after deposition on soils [34]. According to the dissolution kinetics of lead species [9], PbO.PbSO$_4$ would be more available than PbS leading to a possible larger transfer to the biosphere.

Few differences in global composition appear between samples, when observed with XRD. Supplementary phases are present in the finest fraction: 2PbO·PbSO$_4$ in *Furnace* PM$_{2.5-1}$; ZnO only appears in *Refining* PM$_{10-2.5}$ and PM$_{2.5-1}$. Particles collected at this workplace were the only one exhibiting a clear signal for As species. For *Emissions PM*, the same crystallized phases were found within PM$_{tot}$ and PM$_{10-2.5}$, but FeS$_2$ was detected in PM$_{2.5-1}$, only. Chlorine-containing species (Pb(ClO$_4$)$_2$, Cd(ClO$_4$)$_2$) may have been formed from polymer membranes of batteries. Results of metal speciation at individual particle scales obtained by RMS were consistent with those obtained by XRD and EXAFS at bulk scales. Additional species were identified by RMS in *Furnace PM* and *Refining PM*, including PbCO$_3$, Pb$_3$(CO$_3$)$_2$(OH)$_2$, iron oxides (α-Fe$_2$O$_3$, Fe$_3$O$_4$) and CaSO$_4$ (Table 4). Due to the enrichment phenomena previously discussed, a larger variety of species was found by XRD and RMS in size-segregated samples (PM$_{10-2.5}$ and PM$_{2.5-1}$) when compared to PM$_{tot}$. Finally, single particle analysis showed a large chemical heterogeneity that could highly influence the availability of metallic elements.

4.3. Lead exchangeability in function of speciation

Since no obvious relationship was observed between physico-chemical characteristics of particles and their origins or sizes, the soft CaCl$_2$ extraction test appeared to be a preliminary pertinent assay to determine the easily exchangeable metal fraction from particles. The percentage of CaCl$_2$ exchangeable Pb was low (10^{-2} to 10^{-3}, Fig. 3). Assuming that the particles would contain only PbS, PbO, PbSO$_4$ and PbO·PbSO$_4$, this percentage would be less than
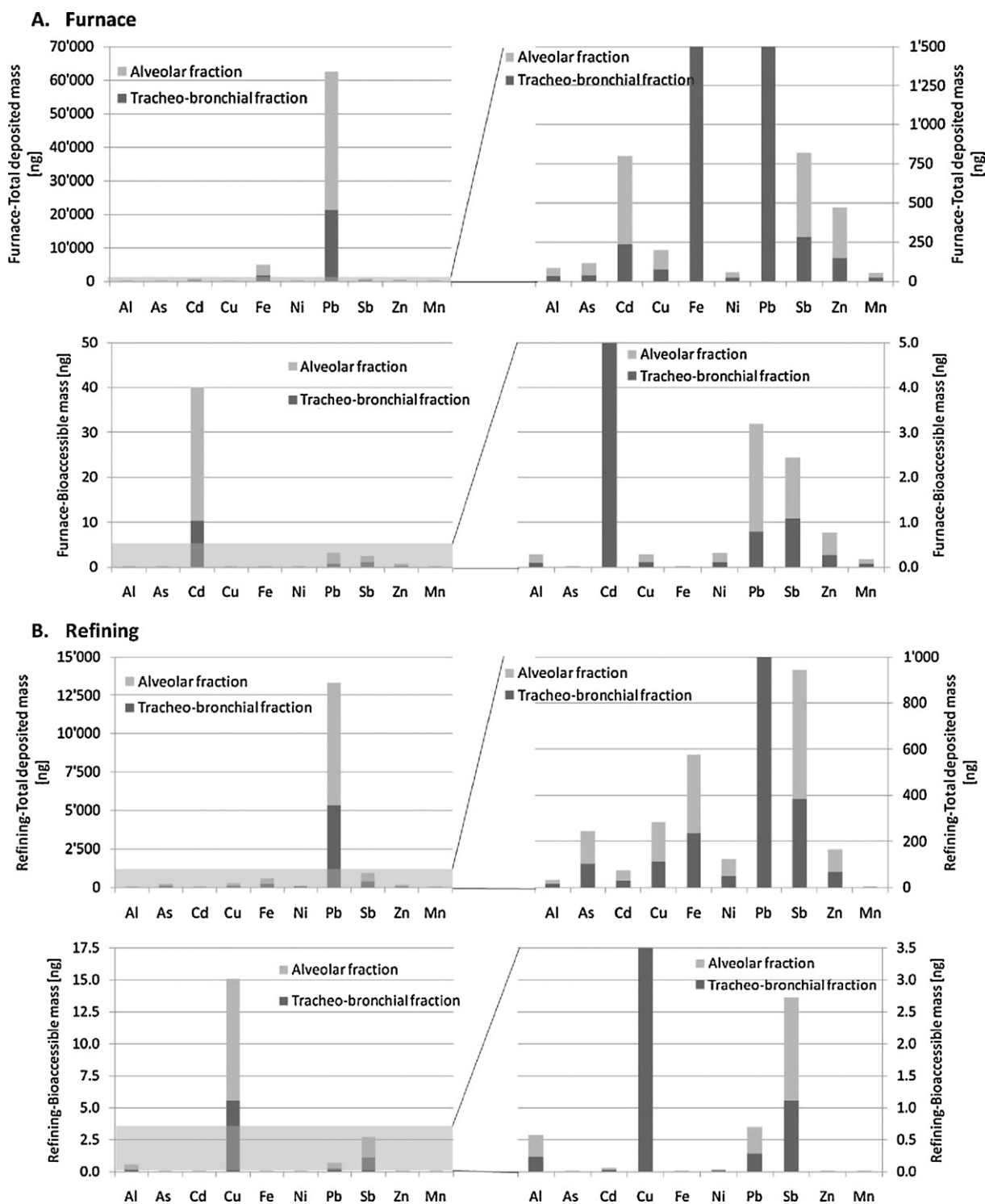
Fig. 4. Total deposited and bioaccessible mass (CaCl$_2$ extraction) of the different elements in the tracheo-bronchial or in the alveolar region calculated for an exposure duration of 8 h at the Furnace (A) or at the Refining (B) workplace. The greyish zone is enlarged on the right panel.

10^{-4}%, as calculated by CHESS [35,36]. Thus, Pb exchangeability is not controlled by the major crystalline Pb species, but probably by altered minerals and sorbed species. Still, due to high Pb contents of particles (up to 45%), Pb concentration in the extractant was relatively high, and particles could not be considered as inert. Moreover, Pb exchangeability is supposed to increase with time, due to particle oxidation and alteration. Recent investigations about metal leaching of PM originating from secondary lead smelter [17] showed that only primary alkaline sulfates and

chlorides (e.g. Na$_3$Pb$_2$(SO$_4$)$_3$Cl and KCl·2PbCl$_2$) could be dissolved readily (in deionized water) and that anglesite (PbSO$_4$) was formed as a final stable alteration product. Anglesite was also detected by XRD in soils exposed to smelter emissions for decades [37]. Other Pb phases found in soils exposed to Pb emissions included Pb sorbed to humic acids and to manganese and iron (oxyhydr)oxide [24,38]. Concerning metals exchangeability, another study on incinerated sludge ashes [39] showed that despite their high Pb and Cu contents (2270 mg kg^{-1} and 2870 mg kg^{-1} respectively), none of these

metals were detected in the MgCl$_2$ (1 M)-extractant. Conversely, Fernandez et al. [40] have shown that 25% and 9% of lead present in urban aerosols collected respectively in Seville and Barcelona were exchanged by MgCl$_2$ (1 M). These contrasted behaviours may be due to different experimental conditions but more likely arise from the composition and structure of particles. In the present study, the percentage of exchangeable metals generally increased with decreasing sizes. This is consistent with a higher sensitivity of smaller particles (governed by the specific particle surface) to weathering processes. This trend was not observed for the two metalloids Sb and As. These metalloids form oxyanions in solution. This fact might induce different ion exchange behaviour as compared to cationic metals. In a previous study, Uzu et al. [10] have demonstrated an increase in soil-plant transfers of lead from process PM$_{10–2.5}$ to PM$_{2.5–1}$ fractions. Ruby et al. [9] showed that bioaccessibility of lead strongly increased for particles below 2.4 μm. An increase in specific surfaces values, inducing greater solid-liquid exchanges between metals in PM and water could explain this phenomenon. It is worth mentioning that the Cu mobilisation by CaCl$_2$ is only observed for *Refining PM*.

4.4. Implications for health risk assessment

Evaluation of health risk due to inhalation of the studied particles is a function of deposited doses and fates after reaching the target organ. We have first to mention that calculated deposited and bioaccessible doses shown in Fig. 4 have to be considered as indicative because we did not consider parameters as variable breathing patterns or clearance processes. In addition, the bioaccessible fraction was estimated by CaCl$_2$ extraction, probably not representative of what could happen in lung lining fluids; nevertheless, it can be considered as a first important step in order to gain information about the fate of metals when deposited in the lungs. With this limitation in mind, our results indicate that the lead lung burden is very important, reaching some tenth of micrograms during each shift. Whereas similar or about half of the French occupational exposure threshold (set at $100 \, \mu g \, m^{-3}$), inhaled levels of lead at both workplaces are of concern and might reach an action level [41].

Compared to the *Refining* place, a larger alveolar deposition of metals is calculated for particles emitted at *Furnace*. Such a difference can be explained by larger amounts of particles of smaller sizes observed at *Furnace* (Table 1). We observed that pulmonary loads with minor elements are not the same at these two workplaces. Workers inhale larger amounts of Cd and Fe at *Furnace* than at *Refining* place. This could be explained by both elements being contaminants found in the incoming batteries processed at *Furnace*. Interestingly, when considering exchangeable fractions, minor elements (Sb, Zn, Ni, Cu and Cd) display higher solubilities than major ones (Fe and Pb). In addition, differences between both workplaces are again observed. At *Furnace*, a relatively large part of inhaled Cd (5%) is easily to dissolve, followed by Ni (0.5%), Mn and Al (0.3%) and Sb (0.16%). High bioaccessible potentials of Cd in addition to larger depositions in the alveolar region, are of concern since this element is classified as probable carcinogenic for humans (IARC group 2A) [42]. On the contrary, at the *Refining* place, it is Cu which is the most soluble element (5%) followed by Al (1.7%) and Sb (0.29%). It is worth mentioning that Cu and Sb are added at this industrial step in order to create particular lead alloys. This adjunction could lead to the formation of chemical species not very stable, thus highly soluble. Cadmium on the contrary is practically not exchangeable in these particles. Immobilisation of Cd could be due to an encapsulation phenomenon, already reported for industrial dusts [41].

In addition, we did the same calculations as for *Emission PM* in order to evaluate the exposure of the plant neighbours. In comparison with workers, these residents would inhale very low quantities of metals (e.g. 400 times less Pb). The bioaccessible fraction is

mainly composed of Cd and Zn, as for particles from *Furnace*. Globally, these bioaccessibility data are in accordance with previous studies using salt extractions and indicating a decreasing leaching order Cd > Cu > Ni > Zn > Sb > Pb > Fe [40,43].

When deposited in lungs, the fate of the different elements will strongly depend on their mobility. Very low exchangeable metals (like Pb or Fe in our study), will probably follow the clearing process of particle itself, either via the mucocilliary escalator (for particles deposited in the tracheo-bronchial compartment) or by macrophage digestion (when deposited in alveoles). Such clearance mechanisms imply that lead particles will be efficiently removed from the lungs and will end in the acidic gastrointestinal tract. Lead bioaccessibility will thus be largely governed by dissolution and uptake processes taking place in the gastro-intestinal tract. On the contrary, the fact that tenth of nanograms of Cd and Cu can be easily dissolved in the alveolar region suggest that acute biological effects induced by such metals are possible in the lungs. It has to be remembered that locally high metal concentrations can be found due to particle deposition and its subsequent partial dissolution.

5. Conclusions and prospects

The present study has highlighted that particles collected at various workplaces of a lead recycling plant were heterogeneous in terms of chemical compositions and Pb speciation. Though containing the same major phases (Pb, PbS, PbO, PbSO$_4$ and PbO·PbSO$_4$), the nature and amount of minor phases differed. Particles also differed by their morphology and size distribution. No simple relationship between metal content or speciation and origin or particle size was observed in our study, probably due to high complexity and heterogeneity of process PM. Moreover, particle composition evolved with time, likely through an atmospheric oxidation.

However, some differences in metal availability were observed between the various particles tested. In particular, metal availability generally increased when particle sizes decreased. Conventional analytical metal measurements in atmospheric particles usually entail the determination of total metal concentrations. Our data clearly show that for sanitary risk evaluation point of view, it could be pertinent to quantify specific metallic forms (species) since bioaccessibility, solubility, geochemical transport and metal cycles largely depend on speciation. Moreover, exposure of workers to other metals in addition to Pb should be taken into account and the effects of multiple contaminations should be further investigated.

Further, it will be necessary to assess bioaccessibility using simulated biological fluids [44] and (eco)toxicity of theses PM to determine their potential consequences on humans and ecosystems.

References

[1] U.S.G. Survey, http://minerals.usgs.gov/ds/2005/140/lead.pdf, 2009.
[2] Citepa, CITEPA, http://www.citepa.org, in, 2009.
[3] V. Ettler, Z. Johan, A. Baronnet, F. Jankovsky, C. Gilles, M. Mihaljevicč, O. Sebek, L. Strnad, P. Bezdicčka, Mineralogy of air-pollution-control residues from a secondary lead smelter: environmental implications, Environ. Sci. Technol. 39 (2005) 9309–9316.

[4] K. Karita, T. Shinozaki, K. Tomita, E. Yano, Possible oral lead intake via contaminated facial skin, Sci. Total Environ. 199 (1997) 125–131.

[5] C. Cloquet, J. Carignan, G. Libourel, T. Sterckeman, E. Perdrix, Tracing source pollution in soils using cadmium and lead isotopes, Environ. Sci. Technol. 40 (2006) 2525–2530.

[6] B. Brunekreef, R.L. Maynard, A note on the 2008 EU standards for particulate matter, Atmos. Environ. 42 (2008) 6425–6430.

[7] U.S.E.P.A. Epa, Particulate Matter (PM2.5) Speciation Guidance, Final Draft, Edition 1, Monitoring and Quality Assurance Group. Emissions, Monitoring and Analysis Division, Office of Air Quality Planning and Standards, 1999.

[8] M.V. Ruby, A. Davis, R. Schoof, S. Eberle, C.M. Sellstone, Estimation of lead and arsenic bioavailability using a physiologically based extraction test, Environ. Sci. Technol. 30 (1996) 422–430.

[9] M.V. Ruby, A. Davis, J.H. Kempton, J.W. Drexler, P.D. Bergstrom, Lead bioavailability – dissolution kinetics under simulated gastric conditions, Environ. Sci. Technol. 26 (1992) 1242–1248.

[10] G. Uzu, S. Sobanska, Y. Aliouane, P. Pradere, C. Dumat, Study of lead phytoavailability for atmospheric industrial micronic and sub-micronic particles in relation with lead speciation, Environ. Pollut. 157 (2009) 1178–1185.

[11] G.l. Uzu, S. Sobanska, G.R. Sarret, M. Muñoz, C. Dumat, Foliar lead uptake by lettuce exposed to atmospheric fallouts, Environ. Sci. Technol. 44 (2010) 1036–1042.

[12] R. Lilis, A. Fischbein, J. Eisinger, Prevalence of lead disease among secondary lead smelter workers and biological indicators of lead exposure, Environ. Res. 14 (1977) 255–285.

[13] T.M. Roberts, T.C. Hutchinson, J. Paciga, A. Chattopadhyay, R.E. Jervis, J. Vanloon, D.K. Parkinson, Lead contamination around secondary smelters: estimation of dispersal and accumulation by humans, Science 186 (1974) 1120–1123.

[14] T.M. Spear, W. Svee, J.H. Vincent, N. Stanisich, Chemical speciation of lead dust associated with primary lead smelting, Environ. Health Perspect. 106 (1998) 565–571.

[15] T.M. Spear, M.A. Werner, J. Bootland, A. Harbour, E.P. Murray, R. Rossi, J.H. Vincent, Comparison of methods for personal sampling of inhalable and total lead and cadmium-containing aerosols in a primary lead smelter, Am. Ind. Hyg. Assoc. J. 58 (1997) 893–1893.

[16] S. Sobanska, N. Ricq, A. Laboudigue, R. Guillermo, C. Bremard, J. Laureyns, J.C. Merlin, J.P. Wignacourt, Microchemical investigations of dust emitted by a lead smelter, Environ. Sci. Technol. 33 (1999) 1334–1339.

[17] V. Ettler, O. Sebek, T.s. Grygar, M. Klementová, P. Bezdicka, H. Slavíková, Controls on metal leaching from secondary Pb smelter air-pollution-control residues, Environ. Sci. Technol. 42 (2008) 7878–7884.

[18] M. Cecchi, C. Dumat, A. Alric, B. Felix-Faure, P. Pradere, M. Guiresse, Multi-metal contamination of a calcic cambisol by fallout from a lead-recycling plant, Geoderma 144 (2008) 287–298.

[19] V.J.G. Houba, I. Novozamsky, T.M. Lexmond, J.J. van der Lee, Applicability of 0.01 M CaCl$_2$ as a single extraction solution for the assessment of the nutrient status of soils and other diagnostic purposes, Commun. Soil Sci. Plant Anal. 21 (1990) 2281–12281.

[20] N.W. Menzies, M.J. Donn, P.M. Kopittke, Evaluation of extractants for estimation of the phytoavailable trace metals in soils, Environ. Pollut. 145 (2007) 121–130.

[21] E. Meers, R. Samson, F.M.G. Tack, A. Ruttens, M. Vandegehuchte, J. Vangronsveld, M.G. Verloo, Phytoavailability assessment of heavy metals in soils by single extractions and accumulation by Phaseolus vulgaris, Environ. Exp. Bot. 60 (2007) 385–396.

[22] Y. Batonneau, C. Bremard, L. Gengembre, J. Laureyns, A. Le Maguer, D. Le Maguer, E. Perdrix, S. Sobanska, Speciation of PM10 sources of airborne nonferrous metals within the 3-km zone of lead/zinc smelters, Environ. Sci. Technol. 38 (2004) 5281–5289.

[23] A. Manceau, M.-C. Boisset, G. Sarret, J.-L. Hazemann, M. Mench, P. Cambier, R. Prost, Direct determination of lead speciation in contaminated soils by EXAFS spectroscopy, Environ. Sci. Technol. 30 (1996) 1540–1552.

[24] G. Morin, J.D. Ostergren, F. Juillot, P. Ildefonse, G. Calas, G.E. Brown, XAFS determination of the chemical form of lead in smelter-contaminated soils and mine tailings; importance of adsorption processes, Am. Mineral. 84 (1999) 420–434.

[25] A.C. Scheinost, S. Abend, K.I. Pandya, D.L. Sparks, Kinetic controls on Cu and Pb sorption by ferrihydrite, Environ. Sci. Technol. 35 (2001) 1090–1096.

[26] Y. Batonneau, J. Laureyns, J.-C. Merlin, C. Bremard, Self-modeling mixture analysis of Raman microspectrometric investigations of dust emitted by lead and zinc smelters, Anal. Chim. Acta 446 (2001) 23–37.

[27] N.S. Li, A.D.R. Lundgren, D. Rovell, Evaluation of six inhalable aerosol samplers, Am. Ind. Hyg. Assoc. J. 61 (2000) 506–516.

[28] ICRP, Human Respiratory Tract Model for Radiological Protection: A Report of a task group of the international commission on radiological protection, International Commission on Radiological Protection, Annals of the ICRP 24, Oxford, Pergamon Press, Publication 66 (1994) 22–23.

[29] CIIT, RIVM, http://www.thehamner.org/mppd/helpfiles/index.htm (accessed; 18.10.2010).

[30] C. Monn, S. Becker, Cytotoxicity and induction of proinflammatory cytokines from human monocytes exposed to fine (PM2.5) and coarse, Toxicol. Appl. Pharmacol. 155 (1999) 245–252.

[31] Y.J. Zhu, N. Olson, T.P. Beebe, Surface chemical characterization of 2.5-mu m particulates (PM2.5) from air pollution in salt lake city using TOF-SIMS, XPS, and FTIR, Environ. Sci. Technol. 35 (2001) 3113–3121.

[32] I.I. Fasfous, T. Yapici, J. Murimboh, N.M. Hassan, C.L. Chakrabarti, M.H. Back, D.R.S. Lean, D.C. Gregoire, Kinetics of trace metal competition in the freshwater environment: some fundamental characteristics, Environ. Sci. Technol. 38 (2004) 4979–4986.

[33] M. Choel, K. Deboudt, P. Flament, G. Lecornet, E. Perdrix, S. Sobanska, Fast evolution of tropospheric Pb- and Zn-rich particles in the vicinity of a lead smelter, Atmos. Environ. 40 (2006) 4439–4449.

[34] P. Bataillard, P. Cambier, C. Picot, Short-term transformations of lead and cadmium compounds in soil after contamination, Eur. J. Soil Sci. 54 (2003) 365–376.

[35] J. Van der Lee, L. Windt, CHESS Tutorial and Cookbook, User's Guide Nr, CIG-Ecole des Mines de Paris, France, 2000.

[36] T. Wolery, CHESS database, EQ3/6: a software Package for Geochemical Modelling of Aqueous Systems: Package Overview and Installation Guide, Technical Report UCRL-MA-110662 PT I ed., Lawrence Livermore National Laboratory, USA.

[37] V. Ettler, A. Vanek, M. Mihaljevic, P. Bezdicka, Contrasting lead speciation in forest and tilled soils heavily polluted by lead metallurgy, Chemosphere 58 (2005) 1449–1459.

[38] F.v. Oort, A.G. Jongmans, L. Citeau, I. Lamy, P. Chevallier, Microscale Zn and Pb distribution patterns in subsurface soil horizons: an indication for metal transport dynamics, Eur. J. Soil Sci. 57 (2006) 154–166.

[39] J.L. Fraser, K.R. Lum, Notes, Availability of elements of environmental importance in incinerated sludge ash, Environ. Sci. Technol. 17 (1983) 52–54.

[40] A.J. Fernandez, M. Ternero, F.J. Barragan, J.C. Jimenez, An approach to characterization of sources of urban airborne particles through heavy metal speciation, Chemosphere – Global Change Sci. 2 (2000) 123–136.

[41] J.C. Rock, A comparison between OSHA-compliance criteria and action-level decision criteria, Am. Ind. Hyg. Assoc. J. 43 (1982) 297–313.

[42] IPCS, Environmental Health Criteria 134, Cadmium (International Program on Chemical Safety), Geneva, WHO, 1992, p. 280.

[43] P. Smichowski, G. Polla, G. Dario, Metal fractionation of atmospheric aerosols via sequential chemical extraction: a review, Anal. Bioanal. Chem. 381 (2004) 302–316.

[44] H. Roussel, C. Waterlot, A. Pelfrêne, C. Pruvot, M. Mazzuca, F. Douay, Cd, Pb and Zn oral bioaccessibility of urban soils contaminated in the past by atmospheric emissions from two lead and zinc smelters, Arch. Environ. Contam. Toxicol. (2009) 945–954.